

**Study of scalar meson production in three
body η_c decays at BABAR**

Antimo Palano

INFN Sezione di Bari, Italy

On behalf of the BABAR Collaboration

Presented results are preliminary

10th International Workshop on Charm Physics (CHARM 2020),
Mexico, May 31-June 4, 2021

Physics motivations

- Charmonium decays can be used to obtain new information on light meson spectroscopy.
- The η_c resonance is strongly coupled to scalar mesons.
- New information can be obtained on the scalar mesons properties and the identification of the scalar glueball.
- The η' meson is supposed to contain a significant gluonic contribution.
(S. D. Bass and P. Moskal, Rev.Mod.Phys.91, 015003 (2019))
- It is of interest to compare η_c decays to:

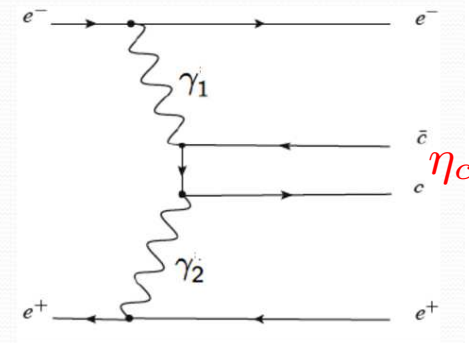
$\eta_c \rightarrow \eta$ (scalar-meson)
 $\eta_c \rightarrow \eta'$ (scalar-meson)

where the scalar meson decays to $\pi^+ \pi^-$ or $K^+ K^-$.

- Compare with results from J/ψ radiative decays.

η_c production in two-photon interactions

- In two-photon interactions we select events in which the e^+ and e^- beam particles are scattered at small angles and remain undetected.



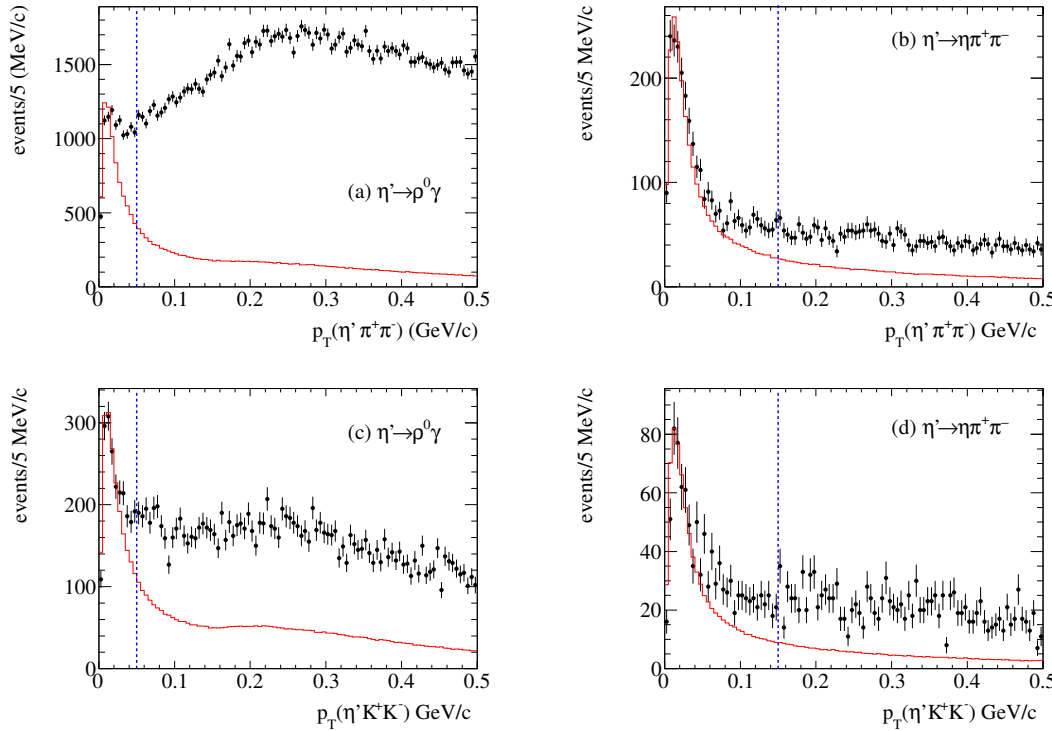
- Only resonances with $J^{PC} = 0^{\pm+}, 2^{\pm+}, 4^{\pm+}$ can be produced.
- We have studied the following final states.

- $\eta_c \rightarrow \eta' \pi^+ \pi^-$, with $\eta' \rightarrow \rho^0 \gamma$ and $\eta' \rightarrow \eta \pi^+ \pi^-$ ($\eta \rightarrow \gamma \gamma$).
- $\eta_c \rightarrow \eta' K^+ K^-$.
- $\eta_c \rightarrow \eta \pi^+ \pi^-$ with $\eta \rightarrow \gamma \gamma$ and $\eta \rightarrow \pi^+ \pi^- \pi^0$.

- Dataset: 519 fb^{-1} recorded with the *BABAR* detector at center-of-mass energies at and near the $\Upsilon(nS)$ ($n = 2, 3, 4$) resonances.

Two-photon signals for $\eta' h^+ h^-$

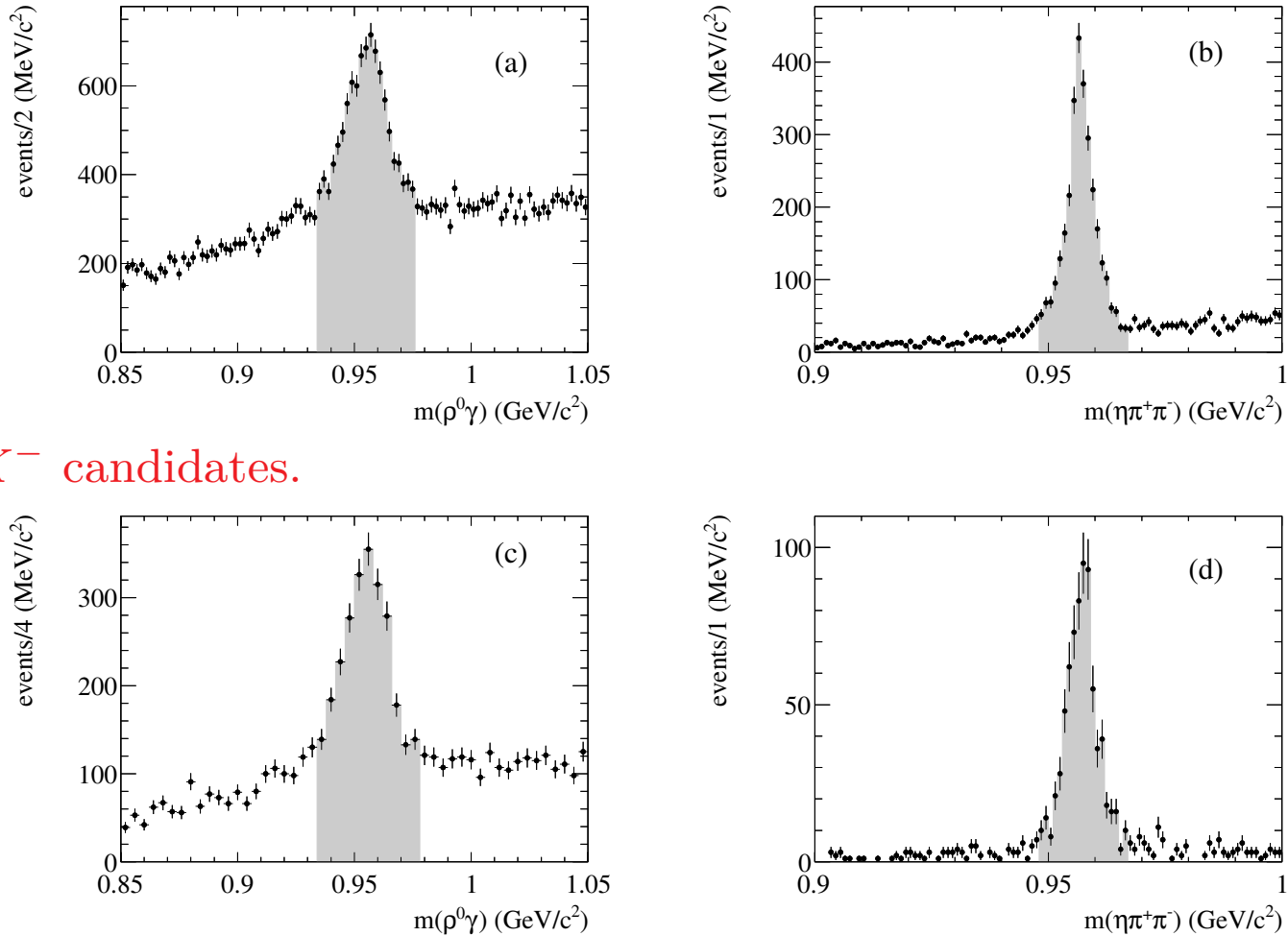
- Removed Initial-State-Radiation $e^+ e^- \rightarrow \gamma_{ISR} \eta' h^+ h^-$ and $\gamma\gamma \rightarrow 4h$ events.
- Two-photon events are isolated from the balance of the transverse momentum p_T with respect to the $e^+ e^-$ direction.
- p_T distributions for $m(\eta' h^+ h^-) > 2.7$ GeV (charmonium region).



- In red are MC simulations normalized to the threshold peak.
- p_T selection optimized on the η_c signal.

η' signals for $\eta_c \rightarrow \eta' h^+ h^-$

$\eta_c \rightarrow \eta' \pi^+ \pi^-$ candidates.

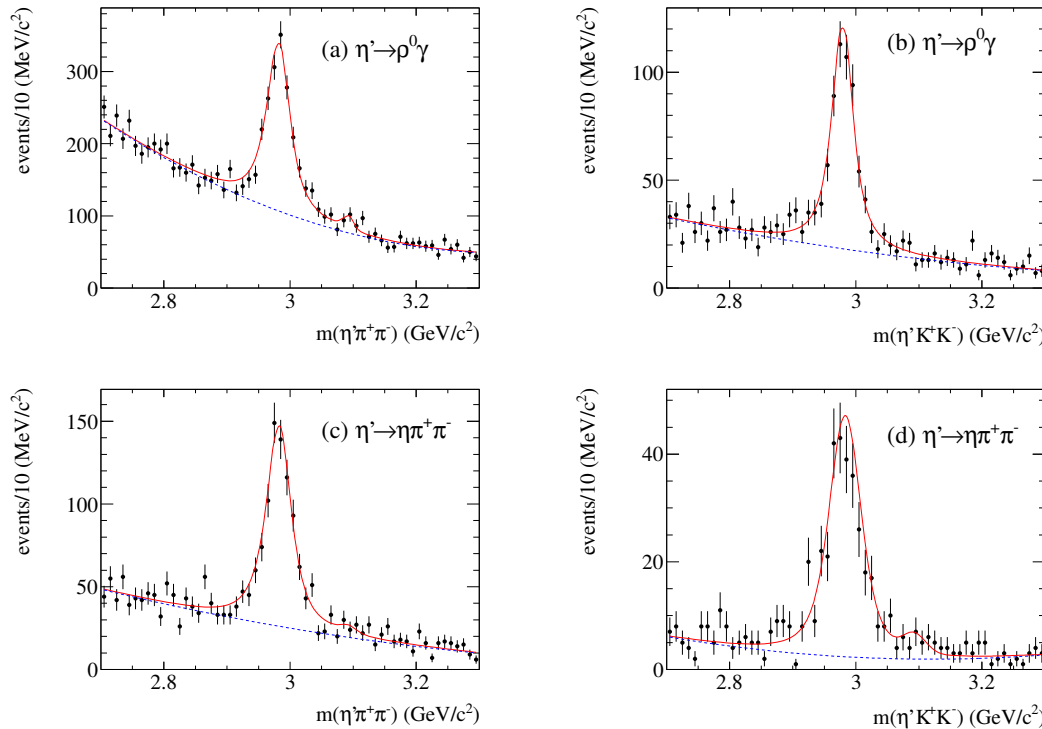


$\eta_c \rightarrow \eta' K^+ K^-$ candidates.

η' reconstructed by adding the decay three-vectors and computing the η' energy using the PDG mass.

η_c signals for $\eta_c \rightarrow \eta' h^+ h^-$

- Mass resolution modeled as the sum of a Gaussian and a Crystal Ball function.
- η_c described by a Breit-Wigner convolved with the experimental resolution.
- Binned χ^2 fits. η_c parameters fixed to PDG values.
- When left free in the fit, parameters consistent with PDG averages.
- Background described by a 2nd order polynomial.



- Included a J/ψ contribution from residual ISR background.
- **First observation of $\eta_c \rightarrow \eta' K^+ K^-$.**

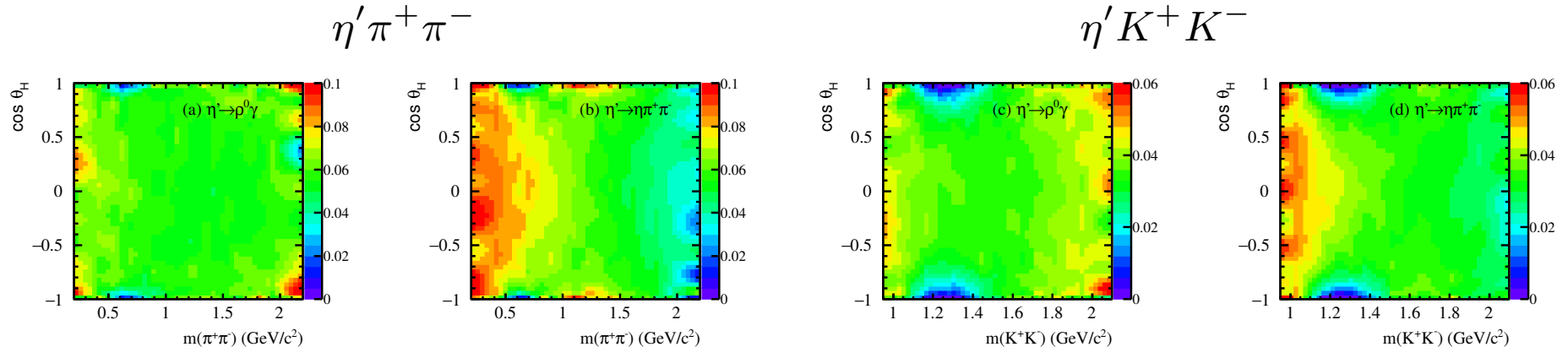
Branching fractions (I)

- We compute the ratio of branching fractions as:

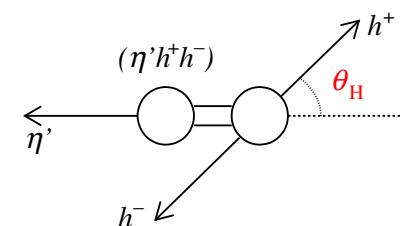
$$\mathcal{R} = \frac{\mathcal{B}(\eta_c \rightarrow \eta' K^+ K^-)}{\mathcal{B}(\eta_c \rightarrow \eta' \pi^+ \pi^-)} = \frac{N_{\eta' K^+ K^-}}{N_{\eta' \pi^+ \pi^-}} \frac{\epsilon_{\eta' \pi^+ \pi^-}}{\epsilon_{\eta' K^+ K^-}}$$

for each η' decay mode.

- $\epsilon_{\eta' K^+ K^-}$ and $\epsilon_{\eta' \pi^+ \pi^-}$ are the corresponding weighted efficiencies.
- The efficiency is projected on the helicity angle $\cos\theta_H$ vs. $m(h^+ h^-)$.
- Fitted using Legendre polynomials in $\cos\theta_H$ and interpolated along $m(h^+ h^-)$.



- Depletions close to $|\cos\theta_H| \approx 1$ due to not reconstructed low momentum particles.
- For a given η' decay mode we apply the same selections to the numerator and denominator, except for particle identification.



Branching fractions (II)

- Each event is weighted by the inverse of the efficiency.
- Background subtraction performed by giving positive weights in the η_c signal region and negative weights in the η_c sidebands.

Final state	yield
$\eta_c \rightarrow \eta' \pi^+ \pi^- (\eta' \rightarrow \rho^0 \gamma)$	$1160 \pm 57 \pm 47$
$\eta_c \rightarrow \eta' K^+ K^-$	$473 \pm 29 \pm 3$
$\eta_c \rightarrow \eta' \pi^+ \pi^- (\eta' \rightarrow \pi^+ \pi^- \eta)$	$619 \pm 35 \pm 11$
$\eta_c \rightarrow \eta' K^+ K^-$	$249 \pm 20 \pm 11$

- We obtain the following values of the branching fractions

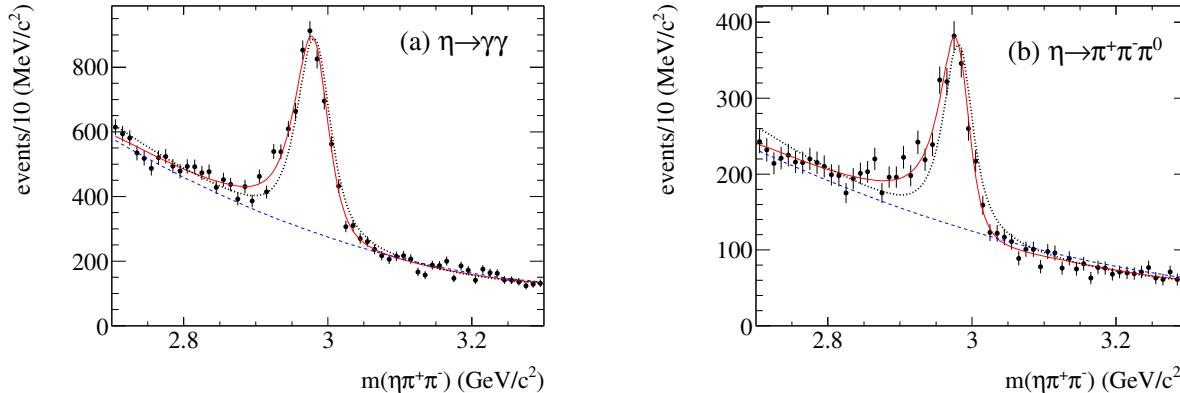
$$\mathcal{R}_1(\rho^0 \gamma) = 0.629 \pm 0.049_{\text{stat}} \pm 0.035_{\text{sys}} \text{ and } \mathcal{R}_2(\eta \pi^+ \pi^-) = 0.672 \pm 0.066_{\text{stat}} \pm 0.078_{\text{sys}}$$

- Average:

$$\mathcal{R} = \frac{\mathcal{B}(\eta_c \rightarrow \eta' K^+ K^-)}{\mathcal{B}(\eta_c \rightarrow \eta' \pi^+ \pi^-)} = 0.644 \pm 0.039_{\text{stat}} \pm 0.032_{\text{sys}}.$$

Study of $\eta_c \rightarrow \eta\pi^+\pi^-$

- $\eta\pi^+\pi^-$ mass spectra for $\eta \rightarrow \gamma\gamma$ and $\eta \rightarrow \pi^+\pi^-\pi^0$.



- The fits to the $\eta\pi^+\pi^-$ mass spectra return η_c masses shifted down by ≈ 10 MeV.
- Fix the η_c parameters and introduce interference between the η_c and the two-photon background

$$f(m) = |A_{nres}|^2 + |A_{res}|^2 + c \cdot 2Re(A_{nres}A_{res}^*)$$

where $|A_{nres}|^2$ is described by a 2nd order polynomial, $A_{res} = \alpha \cdot BW(m) \cdot \exp(i\phi)$.

- We obtain $\chi^2/ndf = 77/54(160/55)$ and $\chi^2/ndf = 46/54(139/55)$ for the two η decay modes, with and without interference.
- **No evidence for interference effects is observed for other η_c to η or η' decay modes.**

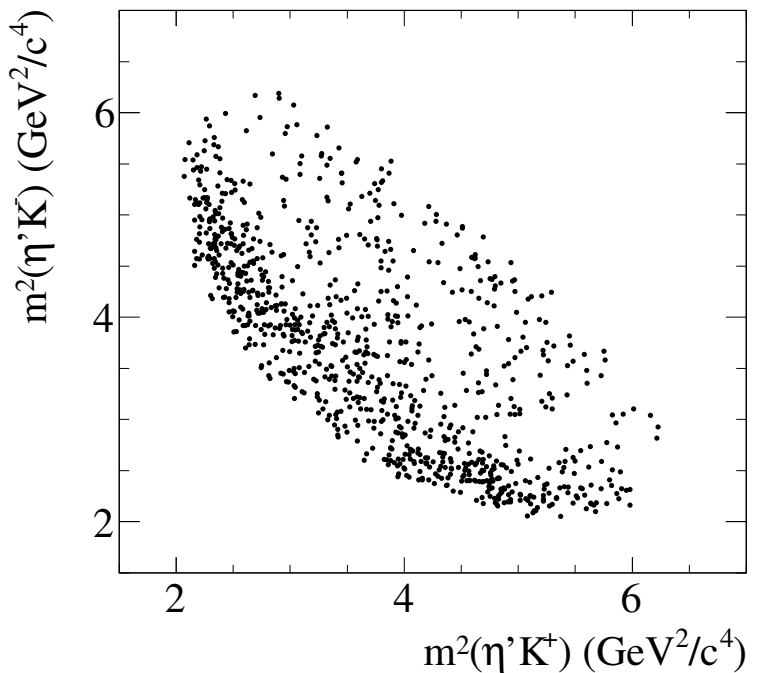
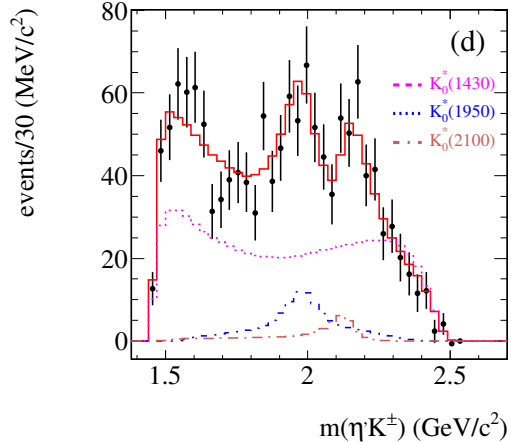
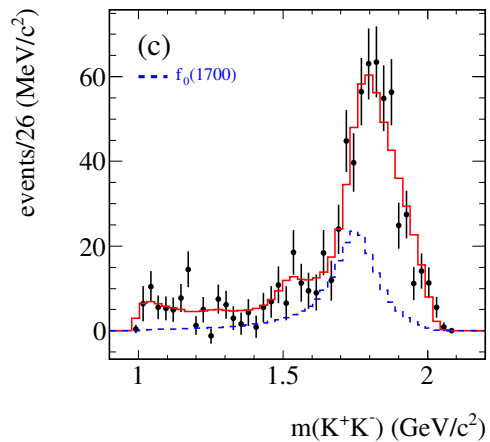
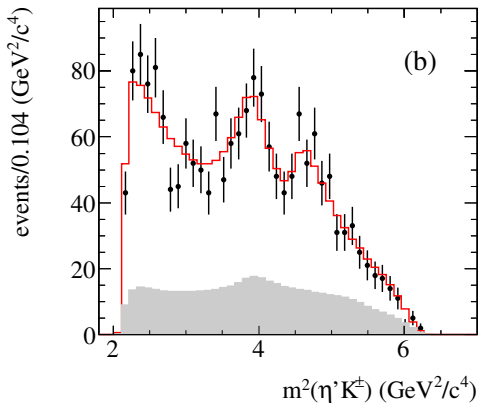
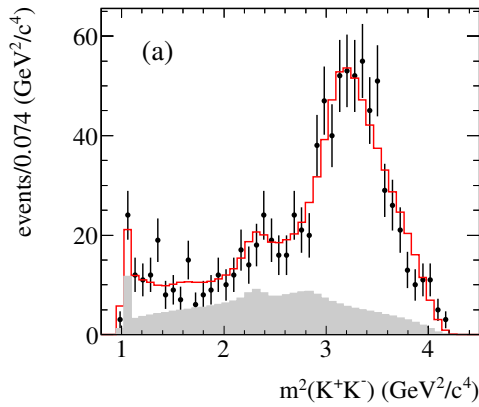
Dalitz plot analysis.

- We perform a Dalitz plot analysis of $\eta_c \rightarrow \eta' \pi^+ \pi^-$, $\eta_c \rightarrow \eta' K^+ K^-$ and $\eta_c \rightarrow \eta \pi^+ \pi^-$ in the η_c mass region using unbinned maximum likelihood fits.
- Efficiencies, normalization integrals and purities are computed separately for the two contributing final states.
- Backgrounds evaluated from the η_c sidebands.
- We scan the likelihood adding resonances one by one and testing the likelihood increase.

Final state	Decay mode	Yield	Fraction (%)	Purity
$\eta_c \rightarrow \eta' K^+ K^-$	$\eta' \rightarrow \rho^0 \gamma$	656	0.705	69.7 ± 1.7
	$\eta' \rightarrow \pi^+ \pi^- \eta$	274	0.295	85.7 ± 2.0
$\eta_c \rightarrow \eta' \pi^+ \pi^-$	$\eta' \rightarrow \rho^0 \gamma$	2239	0.717	51.8 ± 1.1
	$\eta' \rightarrow \pi^+ \pi^- \eta$	883	0.283	69.0 ± 1.6
$\eta_c \rightarrow \eta \pi^+ \pi^-$	$\eta \rightarrow \gamma \gamma$	6512	0.700	58.0 ± 0.6
	$\eta \rightarrow \pi^+ \pi^- \pi^0$	2791	0.300	52.7 ± 1.0

Dalitz plot analysis of $\eta_c \rightarrow \eta' K^+ K^-$

- Combined $\eta' K^+ K^-$ Dalitz plot.
- Mass projections in quadratic and background subtracted linear mass scales.
- Shaded is the fitted background.



- Presence of $f_0(1710)$, $K_0^*(1430)$, $K_0^*(1950)$ and possibly a $K_0^*(2130)$ resonance.

Model for the $K_0^*(1430)$ resonance.

- We describe the $K_0^*(1430)$ resonance using a coupled channel Breit Wigner with couplings to the $K\pi$ and $K\eta'$ final states.

$$BW(m) = \frac{1}{m_0^2 - m^2 - i(\rho_1(m)g_{\pi K}^2 + \rho_2(m)g_{\eta' K}^2)},$$

where $\rho_i(m) = 2P/m$ and $\rho_2(m)$ becomes imaginary below the $K\eta'$ threshold.

- We obtain the $K_0^*(1430)$ parameters from a fit to the $K\pi$ S-wave from $\eta_c \rightarrow K\bar{K}\pi$.

$$\text{S-wave}(m) = B(m) + c \cdot BW_{K\pi}(m)e^{i\phi},$$

where $B(m) = \rho_1(m)e^{-\alpha m}$.

- Combined $K_S^0 K\pi$ and $K^+ K^- \pi^0$ data from BaBar.

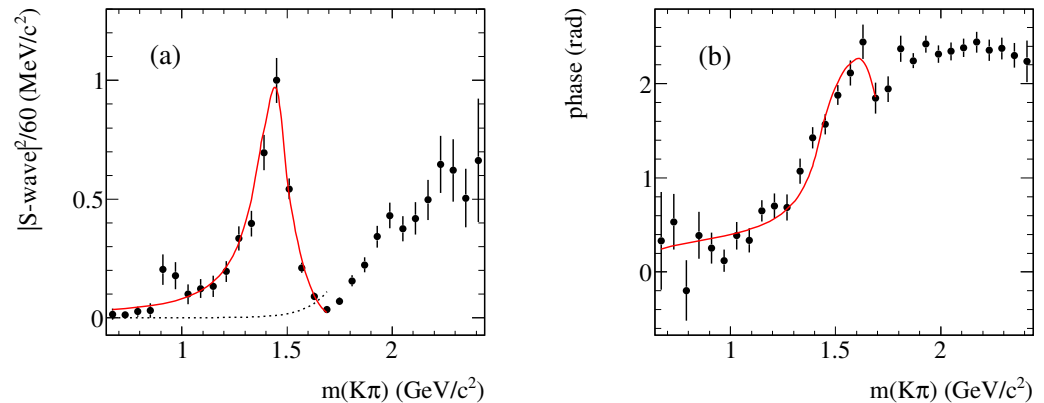
(J.P. Lees et.al., Phys. Rev. D 93, 012005 (2016).)

$$m_0 = 1447 \pm 8 \text{ MeV},$$

$$g_{K\pi}^2 = 0.414 \pm 0.026 \text{ GeV}^2/c^4,$$

$$g_{K\eta'}^2 = 0.197 \pm 0.105 \text{ GeV}^2/c^4,$$

$$\frac{g_{K\eta'}^2}{g_{K\pi}^2} = 0.476 \pm 0.254.$$



Results from the Dalitz plot analysis of $\eta_c \rightarrow \eta' K^+ K^-$

- Using the above $K_0^*(1430)$ parameters we obtain the following fractions and relative phases.

Final state	fraction (%)	phase (rad)
$f_0(1710)\eta'$	$30.0 \pm 5.3 \pm 1.6$	0.
$K_0^*(1430)^+ K^-$	$57.6 \pm 7.5 \pm 2.1$	$0.79 \pm 0.13 \pm 0.59$
$K_0^*(1950)^+ K^-$	$7.3 \pm 2.8 \pm 0.4$	$1.09 \pm 0.23 \pm 1.10$
$f_0(1500)\eta'$	$0.9 \pm 1.0 \pm 0.3$	$0.24 \pm 0.51 \pm 0.10$
$f_0(980)\eta'$	$4.8 \pm 3.0 \pm 0.4$	$-0.92 \pm 0.53 \pm 0.05$
$f_2(1270)\eta'$	$2.7 \pm 1.4 \pm 0.1$	$2.9 \pm 0.42 \pm 0.09$
$K_0^*(2130)^+ K^-$	$2.7 \pm 1.7 \pm 0.4$	$-0.48 \pm 0.38 \pm 0.06$
sum	$105.9 \pm 10.4 \pm 2.7$	

- Leaving free the $g_{K\eta'}$ parameter, we obtain $g_{K\eta'}^2 = 0.113 \pm 0.279 \text{ GeV}^2/c^4$.
- We also leave free other resonances parameters and obtain:

Resonance	Mass (MeV/ c^2)	Γ (MeV)	significance ($n\sigma$)
$f_0(1710)$	$1757 \pm 24 \pm 9$	$175 \pm 23 \pm 4$	8.2
$K_0^*(1950)$	$1979 \pm 26 \pm 3$	$144 \pm 44 \pm 21$	4.5
$K_0^*(2130)$	$2128 \pm 31 \pm 9$	$95 \pm 42 \pm 76$	3.1

- We obtain $\chi^2/ndf = 281/262 = 1.1$ on the $(m(K^+ K^-), \cos\theta_H)$ plane, and $ndf = N_{cells} - N_{par}$.
- Non-Resonant contribution consistent with zero.

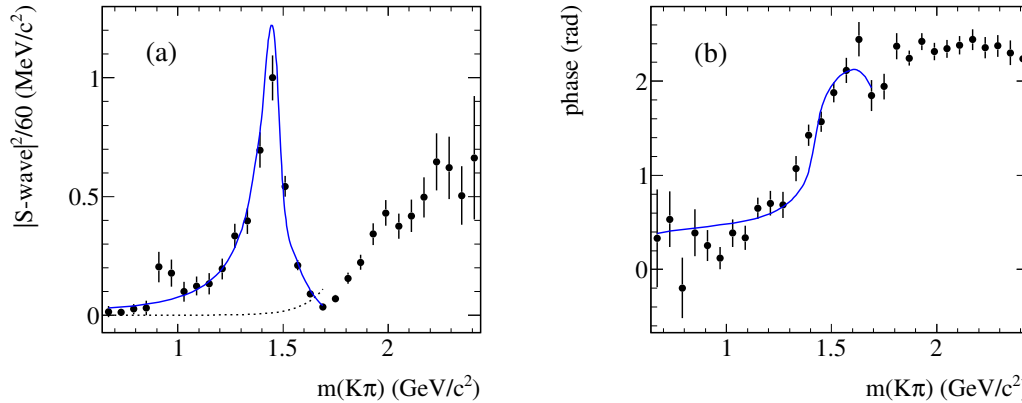
Measurement of the relative $K_0^*(1430) \rightarrow \eta' K$ coupling (I)

- We obtain a better precision estimate of $\frac{g_{K\eta'}^2}{g_{K\pi}^2}$ combining previous measurements with present data and using an iterative procedure.
- Belle: $\Gamma_{\gamma\gamma}\mathcal{B}(\eta_c \rightarrow \eta'\pi^+\pi^-) = 65.4 \pm 2.6_{\text{stat}} \pm 7.8_{\text{sys}}$ eV,
Q. N. Xu et al., Phys.Rev.D98, 072001 (2018)
- BaBar: $\Gamma_{\gamma\gamma}\mathcal{B}(\eta_c \rightarrow K\bar{K}\pi) = 386 \pm 0.008_{\text{stat}} \pm 0.021_{\text{sys}}$ eV,
P. del Amo Sanchez et al. Phys.Rev.D84, 012004 (2011)
- Present analysis: $\mathcal{R} = \frac{\mathcal{B}(\eta_c \rightarrow \eta' K^+ K^-)}{\mathcal{B}(\eta_c \rightarrow \eta' \pi^+ \pi^-)} = 0.644 \pm 0.039_{\text{stat}} \pm 0.032_{\text{sys}}$
- BaBar Dalitz plot analysis of $\eta_c \rightarrow K^+ K^- \pi^0$:
 $\mathcal{B}(\eta_c \rightarrow K^- K_0^*(1430)^+ (\rightarrow \pi^0 K^+)) = (33.8 \pm 1.9_{\text{stat}} \pm 0.4_{\text{sys}})\%$
- Present Dalitz plot analysis of $\eta_c \rightarrow \eta' K^+ K^-$:
 $\mathcal{B}(\eta_c \rightarrow K_0^*(1430)^+ K^-) = (57.6 \pm 7.5 \pm 2.1)\%$
- Combining the above information obtain: $\frac{g_{\eta' K}^2}{g_{\pi K}^2} = 1.56 \pm 0.26_{\text{stat}} \pm 0.23_{\text{sys}}$
- To be compared with the measurement from the $K\pi$ S-wave: $\frac{g_{K\eta'}^2}{g_{K\pi}^2} = 0.476 \pm 0.254$

Measurement of the relative $K_0^*(1430) \rightarrow \eta' K$ coupling (II)

□ To solve this discrepancy:

- Refit the $K\pi$ S-wave with fixed $\frac{g_{\eta' K}^2}{g_{\pi K}^2} = 1.56$ value. $\chi^2/ndf = 74/32 (=34/32$ inc.sys.).



- Refit the $\eta_c \rightarrow \eta' K^+ K^-$ using the resulting new $K_0^*(1430)$ parameters and obtain a new value of $\mathcal{B}(\eta_c \rightarrow K_0^*(1430)^+ K^-) = (69.9 \pm 9.2 \pm 2.6)\%$ with similar fit quality.

□ We obtain

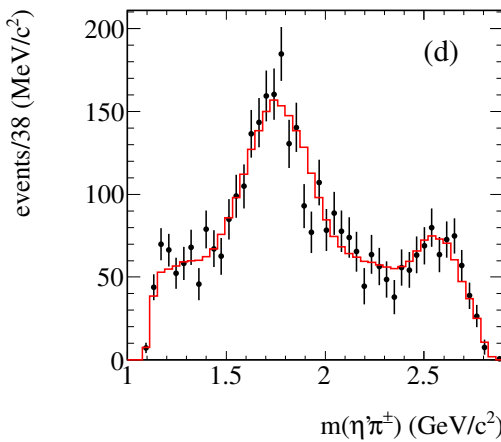
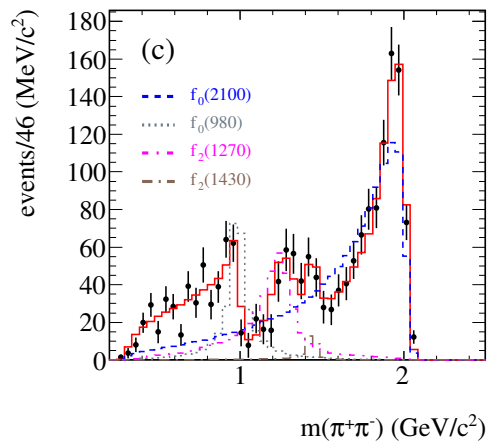
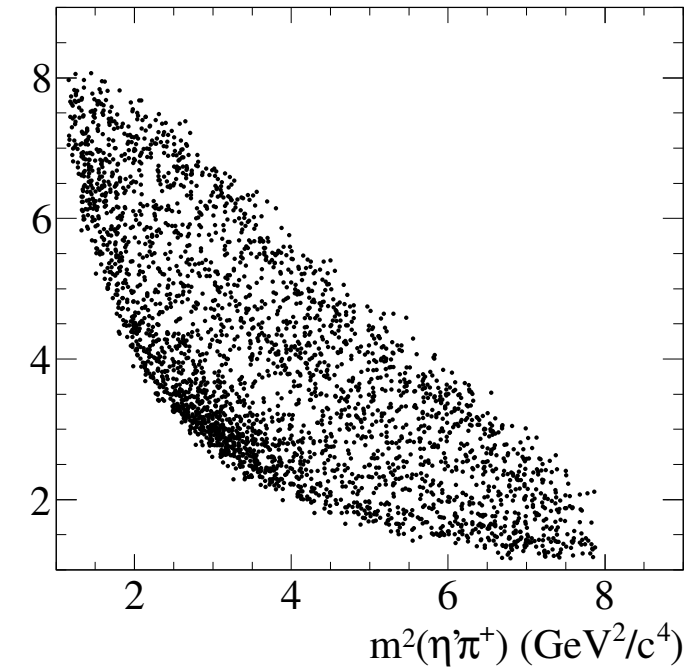
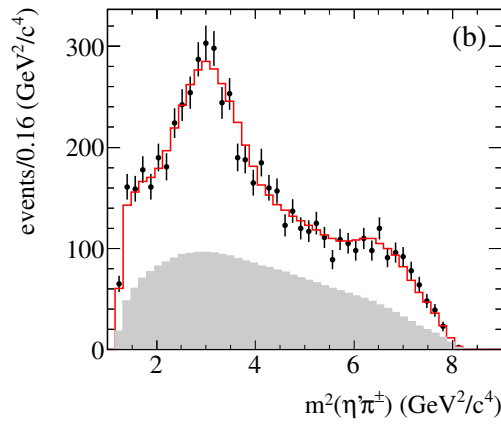
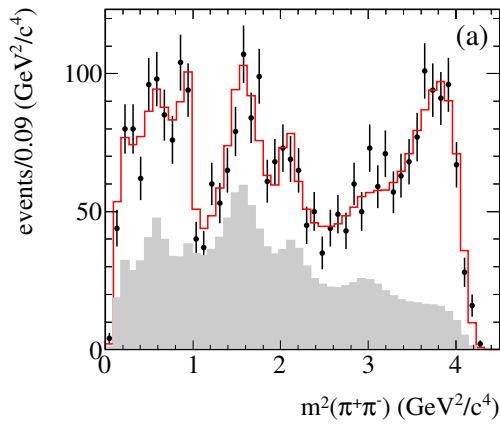
$$m(K_0^*(1430)) = 1453 \pm 22_{\text{stat}} \pm 6_{\text{sys}} \text{ MeV}/c^2,$$

$$g_{K\pi}^2 = 0.462 \pm 0.036_{\text{stat}} \pm 0.048_{\text{sys}} \text{ GeV}^2/c^4,$$

$$\frac{g_{\eta' K}^2}{g_{\pi K}^2} = 1.66 \pm 0.27_{\text{stat}} \pm 0.29_{\text{sys}}.$$

Dalitz plot analysis of $\eta_c \rightarrow \eta' \pi^+ \pi^-$

- Combined $\eta' \pi^+ \pi^-$ Dalitz plot.
- Mass projections in quadratic and background subtracted linear mass scales.



- Decay dominated by the $f_0(2100) \rightarrow \pi^+ \pi^-$ resonance.

Results from the Dalitz plot analysis of $\eta_c \rightarrow \eta' \pi^+ \pi^-$

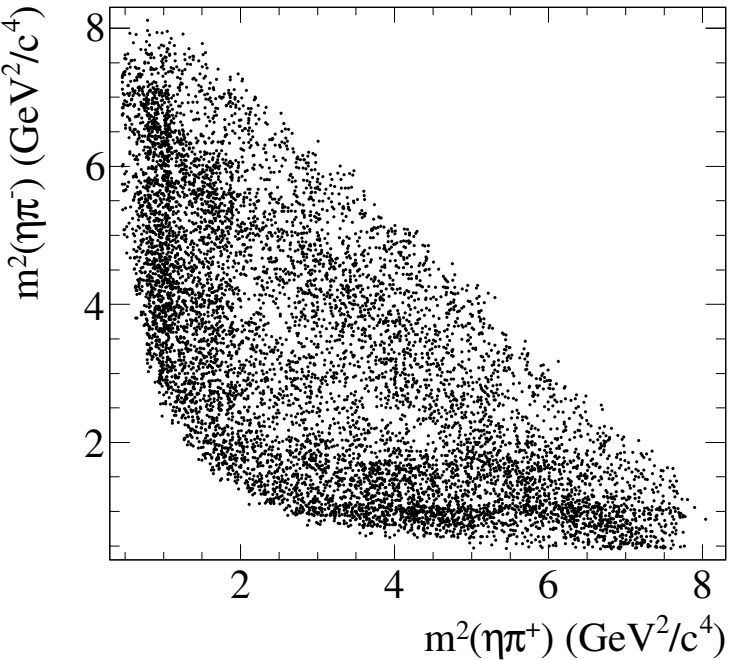
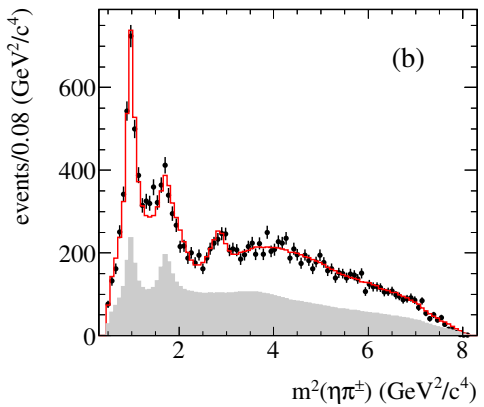
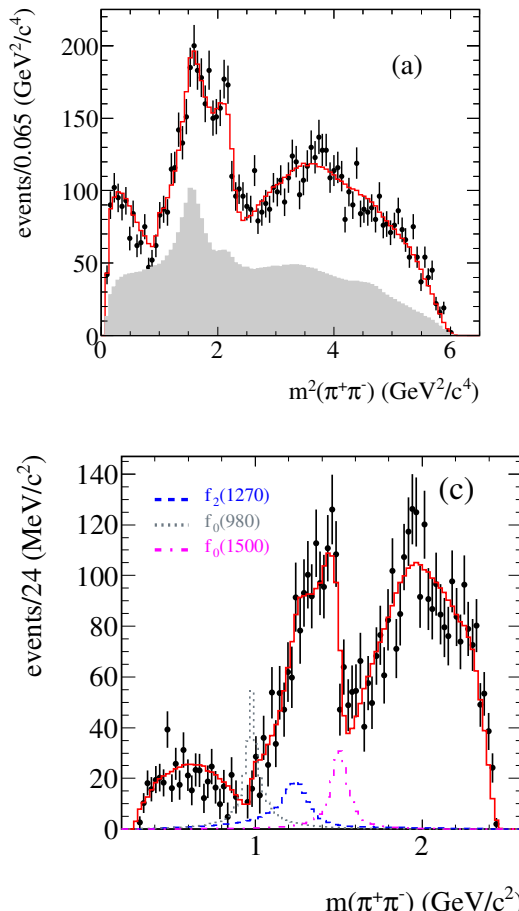
Final state	fraction (%)	phase (rad)
$f_0(2100)\eta'$	$74.9 \pm 7.5 \pm 3.6$	0.
$f_0(500)\eta'$	$4.3 \pm 2.3 \pm 0.7$	$-5.89 \pm 0.24 \pm 0.10$
$f_0(980)\eta'$	$16.1 \pm 2.4 \pm 0.5$	$-5.31 \pm 0.16 \pm 0.04$
$f_2(1270)\eta'$	$22.1 \pm 2.9 \pm 2.4$	$-3.60 \pm 0.16 \pm 0.03$
$f_2(1430)\eta'$	$1.9 \pm 0.7 \pm 0.1$	$-2.45 \pm 0.32 \pm 0.11$
$a_2(1710)\pi$	$3.2 \pm 1.9 \pm 0.5$	$-0.75 \pm 0.27 \pm 0.11$
$a_0(1950)\pi$	$2.5 \pm 1.1 \pm 0.1$	$-0.02 \pm 0.32 \pm 0.06$
$f_2(1800)\eta'$	$5.3 \pm 2.2 \pm 1.4$	$0.67 \pm 0.24 \pm 0.08$
sum	$130.5 \pm 9.5 \pm 4.7$	

- Non-Resonant contribution consistent with zero. $\chi^2/ndf = 409/386 = 1.1$
- We leave free the parameters of the $f_0(500)$, $f_2(1430)$, and $f_0(2100)$.
- The $f_0(2100)$ parameters are consistent with BESIII values in $J/\psi \rightarrow \gamma \eta \eta$
(M. Ablikim *et al.*, Phys. Rev. D **87**, 092009 (2013).)

Resonance	Mass (MeV/ c^2)	Γ (MeV)	significance ($n\sigma$)
$f_0(500)$	953 ± 90	335 ± 81	
$f_2(1430)$	$1440 \pm 11 \pm 3$	$46 \pm 15 \pm 5$	4.8
$f_0(2100)$	$2116 \pm 27 \pm 17$	$289 \pm 34 \pm 15$	10

Dalitz plot analysis of $\eta_c \rightarrow \eta\pi^+\pi^-$

- Combined $\eta\pi^+\pi^-$ Dalitz plot.
- Mass projections in quadratic and background subtracted linear mass scales.



- Complex resonant structures both in signal and background regions.
- A new $a_0(1700) \rightarrow \eta\pi$ resonance.

Results from the Dalitz plot analysis of $\eta_c \rightarrow \eta\pi^+\pi^-$

Final state	fraction (%)	phase (rad)
$a_0(980)\pi$	$12.3 \pm 1.2 \pm 0.9$	0.
$a_2(1310)\pi$	$2.5 \pm 0.7 \pm 0.6$	$-1.04 \pm 0.13 \pm 0.20$
$f_0(500)\eta$	$4.3 \pm 1.3 \pm 0.7$	$0.54 \pm 0.14 \pm 0.20$
$f_2(1270)\eta$	$4.6 \pm 0.9 \pm 0.4$	$-1.15 \pm 0.11 \pm 0.05$
$f_0(980)\eta$	$5.7 \pm 1.3 \pm 1.0$	$-2.41 \pm 0.09 \pm 0.04$
$f_0(1500)\eta$	$4.2 \pm 0.7 \pm 0.6$	$2.32 \pm 0.13 \pm 0.05$
$a_0(1450)\pi$	$15.0 \pm 2.4 \pm 2.1$	$2.60 \pm 0.09 \pm 0.11$
$a_0(1700)\pi$	$3.5 \pm 0.8 \pm 0.6$	$1.39 \pm 0.15 \pm 0.12$
$f_2(1950)\eta$	$4.2 \pm 1.0 \pm 0.6$	$-1.59 \pm 0.15 \pm 0.20$
sum	$56.3 \pm 3.7 \pm 2.9$	
NR	$172.7 \pm 8.0 \pm 10.0$	$1.67 \pm 0.07 \pm 0.03$

□ χ^2 on the $(m(\pi^+\pi^-), \cos\theta_H)$ plane gives $\chi^2/ndf = 419/382 = 1.1$.

□ A new $a_0(1700)$ resonance is observed in the $\eta\pi^\pm$ mass spectrum, with fitted parameters:

$$m = 1704 \pm 5 \pm 2 \text{ MeV}, \Gamma = 110 \pm 15 \pm 11 \text{ MeV}, n\sigma = 8$$

□ Large Non-Resonant contribution, possibly related to the η_c interference with the two-photon background.

Summary.

- First observation of $\eta_c \rightarrow \eta' K^+ K^-$ and measurement of its branching fraction.
- Observation of a new $a_0(1700) \rightarrow \eta \pi$ resonance.
- Evidence for $f_2(1430) \rightarrow \pi^+ \pi^-$.
- Comparison between the fractional contributions in η_c decays to gluonium candidates for final states involving η or η' meson.

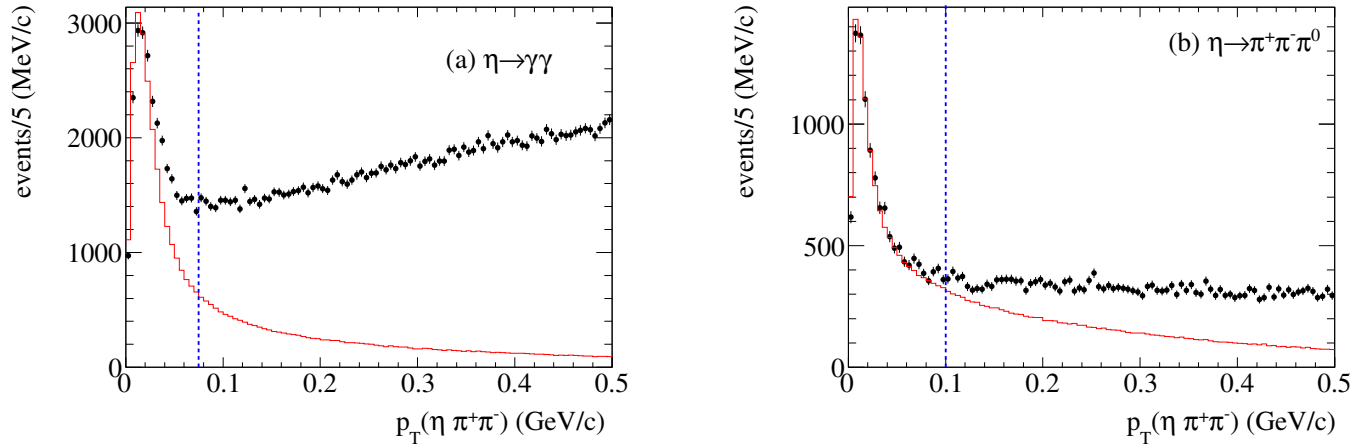
Final state	$f_0(1500)(\%)$	$f_0(1710)(\%)$	$f_0(2100)(\%)$
$\eta K^+ K^-$	$23.7 \pm 7.0 \pm 1.8$	$8.9 \pm 0.2 \pm 0.4$	
$\eta \pi^+ \pi^-$	$4.2 \pm 0.7 \pm 0.6$		0.
$\eta' K^+ K^-$	$0.9 \pm 1.0 \pm 0.3$	$30 \pm 5.3 \pm 1.6$	
$\eta' \pi^+ \pi^-$	0.3 ± 0.2		$74.9 \pm 7.5 \pm 3.5$

- We observe an enhanced contributions of $f_0(1710)$ and $f_0(2100)$ in η_c decays to η' .
- This effect may point to an enhanced gluonium content in the $f_0(1710)$ and $f_0(2100)$ resonances.
- A similar conclusion is drawn in the study of $J\psi$ radiative decays by BESIII.
- **The results obtained in this analysis allow to add the $f_0(2100)$ resonance in the list of the candidates for the scalar glueball.**

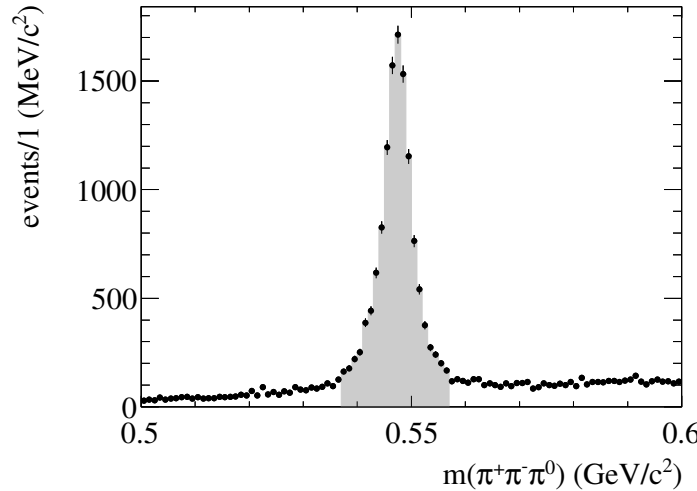
Backup slides

Reconstruction of $\eta_c \rightarrow \eta\pi^+\pi^-$

- p_T distributions and $\eta\pi^+\pi^-$ mass spectra for $\eta \rightarrow \gamma\gamma$ and $\eta \rightarrow \pi^+\pi^-\pi^0$.



- $\pi^+\pi^-\pi^0$ mass spectrum for $\eta\pi^+\pi^-$ candidates with $\eta \rightarrow \pi^+\pi^-\pi^0$.



Full mass spectra

